ISSN 1672-9145 **Acta Biochimica et Biophysica Sinica** 2007, **39**(10): 751–762 **CN** 31-1940/Q

Cell Transformation and Proteome Alteration in QSG7701 Cells Transfected with Hepatitis C Virus Non-structural Protein 3

Qiongqiong HE[1,2,3], Ruixue CHENG[1], Zhuchu CHEN[2,3], Xuxian XIAO[4], Zhiqiang XIAO[2], Cui LI[2], Bo LI[1], Pengfei ZHANG[2], Hui ZHENG[1], and Deyun FENG[1]*

[1] *Department of Pathology, Basic Medical College, Central South University, Changsha 410078, China;*
[2] *Key Laboratory of Cancer Proteomics, Ministry of Health of China, Xiangya Hospital, Central South University, Changsha 410078, China;*
[3] *Cancer Research Institute, Central South University, Changsha 410078, China;*
[4] *Research Center of Medical Chemistry, Central South University, Changsha 410078, China*

Abstract Persistent hepatitis C virus (HCV) infection can cause liver cirrhosis and hepatocellular carcinoma. Non-structural protein 3 (NS3), an important part of HCV, has been implicated in the life cycle of the virus and interacts with host cellular proteins. In this study, we investigated the effect of NS3 protein on cell tranformation and related protein alteration in human hepatocyte QSG7701 cells. The results indicated that stable expression of the NS3 protein in QSG7701 cells induced transformed characters with reduced population doubling time, anchorage-independent growth and tumor development. Fifteen differentially-expressed proteins were separated and identified using 2-D electrophoresis and matrix-assisted laser desorption ionization-time of flight mass spectrometry. Western blot analysis confirmed that the increase of phospho-p44/42 and phospho-p38 proteins was associated with transformed cells. These results supported the view that HCV NS3 protein plays a transforming role and provided some clues to elucidate the carcinogenesis mechanism of HCV-related hepatocellular carcinoma.

Keywords liver neoplasm; hepatitis C virus; viral non-structural protein; cell transformation; proteomics

It is estimated that approximately 400 million people, or more than 2% of the world's population, are infected with hepatitis C virus (HCV). Persistent HCV infection often leads to chronic hepatitis that can result in liver cirrhosis and hepatocellular carcinoma (HCC) [1,2]. In spite of increasing evidence about immunologically-mediated and virus-induced mechanisms, so far the origin of hepatocarcinogenesis in HCV infection remains poorly defined [3].

HCV has a positive-strand RNA genome of approximately 9.4 kb that serves as a template for replication and for translation of a polyprotein of 3010–3033 amino acids. The polyprotein is cleaved co- and post-translationally by host and viral proteases into at least 10 different mature proteins in the order NH2-C-E1-E2-p7-NS2-NS3-NS4A-NS4B-NS5B-COOH [4]. One of these proteins, non-structural protein 3 (NS3) with 631 amino acid residues, is indispensable for virus replication. Multiple enzymatic activities are associated with the NS3 protein, such as serine protease, RNA-stimulated nucleoside triphosphatase, and RNA helicase activities. The catalytic domain of the chymotrypsin-like NS3 protease, comprised of 181 amino acids, has been mapped to the NH2-terminal region of the protein, whereas the nucleoside triphosphatase and the helicase are located within the COOH-terminal 450 amino acids of NS3 [5].

Several studies have pointed out controversial roles for the NS3 protein in cell proliferation and transformation. It was reported that the NS3 protein could double the growth rate of NIH3T3 cells and induce tumor in nude mice when NS3 is expressed constitutively [6,7]. HCV NS3 could suppress cell apoptosis induced by actinomycin D [8]. Further research showed that the HCV NS3 serine protease was involved in rat fibroblast cell transformation and that the ability to transform required an active enzyme [9]. NS3-

Received: April 19, 2007 Accepted: June 7, 2007
This work was supported by the grants from the National Natural Science Foundation of China (Nos. 30270601 and 30671846)
*Corresponding author: Tel, 86-731-4327291; Fax, 86-731-2650408; E-mail, dyfeng743@sohu.com

DOI: 10.1111/j.1745-7270.2007.00344.x

specific single-chain antibodies could shuttle NS3 from the cytosol to the nucleus with concomitant inhibition of cell proliferation and loss of the transformed phenotype [10]. In contrast, other studies revealed HCV NS3 expression inhibited the growth of Huh7 and Hep3B cells, and these cells were arrested in the G_2/M phase of the cell cycle [11]. HCV NS3 promoted caspase-8-induced apoptosis at a pathway site distal to Fas-associated death domain, and NS3 might represent a new class of pro-apoptotic proteins [12]. All these reports were based on *in vitro* systems in non-hepatic cell lines of animal origin, or hepatoma cells, and the discrepancies in their results might be due to the different experimental settings. As HCV is a hepatotropic virus, it is more appropriate to use a hepatocyte with normal phenotype to study the effects of the HCV NS3 protein.

In terms of its pathogenesis, the HCV NS3 protein was shown to strongly modulate the activity of protein kinases C and A, and prevent the protein kinases from interacting with their intracellular target proteins *in vivo* [13,14]. The HCV NS3 protein can specifically repress p21waf1/cip1 promoter activity [7], activate the mitogen-activated (MAPK) signalling pathway JNK [15], and enhance telomerase activity [16]. Because of the limitations in conventional techniques, researchers have been restricted to only a few biological parameters and target molecules at a time, and little has been known regarding the specific alterations responsible for the development or progression of HCV infection. Nowadays, the proteomic approach is considered to be the key technology in the global analysis of protein expression and in the understanding of gene function. Proteomic analysis was recently applied to tissue or cell samples to find molecular markers or tumor-specific and tumor-associated proteins for HCV-associated HCC [17,18]. However, the comprehensive analysis of protein alteration to investigate the mechanism of HCC induced by HCV infection has rarely been done.

In the present work, a hepatic cell line of human origin (QSG7701) was selected to transfect with HCV NS3. Cell growth assay and anchorage-independent growth and tumor development in nude mice were applied to investigate the change of biological behaviors. High throughput techniques of proteomic analysis combining 2-D electrophoresis (2-DE) and matrix-assisted laser desorption ionization-time of flight mass spectrometry (MALDI-TOF MS) with a bioinformatics database were used to identify differentially-expressed proteins. Western blot analysis further validated two up-regulated proteins of p44/42 and p38. The pathological significance of the differentially-expressed proteins is discussed.

Materials and Methods

Cell culture

The human hepatocyte cell line QSG7701 [19] was obtained from the Cell Bank of Type Culture Collection of Chinese Academy of Sciences, Shanghai Institutes for Biological Sciences, Chinese Academy of Sciences (Shanghai, China), and the HepG2 cell line was obtained from American Type Culture Collection (Manassas, USA). Cells were maintained in Dulbecco's modified Eagle's medium supplemented with 10% fetal calf serum, 100 U/ml penicillin G, and 50 μg/ml streptomycin, at 37 ºC in a humidified atmosphere of 5% CO_2. All cell culture reagents were from Gibco BRL (Carlsbad, USA).

Expression vectors

Mammalian expression vector pRcHCNS3-5' expressing HCV NS3 C-terminal truncated protein was kindly provided by Prof. TAKEGAMI (Kanazawa Medical University, Ishikawa, Japan) [6]. Non-expressive plasmid pRcCMV was purchased from Sigma-Aldrich (St. Louis, USA).

Transfections

Plasmid pRcHCNS3-5' was introduced into QSG7701 cells according to the instructions supplied with Lipofectamine reagent (Gibco BRL). Cells were seeded into selection medium containing 400 μg/ml G418 until several G418-resistant clones (pRcHCNS3/QSG) were established, then the cells were maintained in G418 with a concentration of 200 μg/ml. The clones constitutively expressing HCV NS3 protein were validated by polymerase chain reaction (PCR) and Western blot analysis. QSG7701 cells were also transfected with the non-expression vector pRcCMV as a negative control (pRcCMV/QSG). QSG7701 parental cells were used for the parallel control.

PCR analysis

To detect cDNA in stable transfectants, total genomic DNA was extracted according to standard methods and quantified with an ultraviolet spectrophotometer. DNA PCR was carried out using primers (sense: 5′-CGGGCACG-TTGTAGGCATC-3′, antisense: 5′-AACGGACGGCTT-TAGGACGA-3′) and a reaction consisted of 1 cycle of 90 ºC for 90 s, followed by 35 cycles of 94 ºC for 30 s, 57 ºC for 30 s, 72 ºC for 40 s, then 72 ºC for 5 min. PCR products were subjected to electrophoresis on a 0.8 % agarose gel, visualized by EB staining.

Western blot analysis

Cells were collected by centrifugation at 3000 *g* for 4 min at 4 ºC, washed twice in phosphate-buffered saline (PBS) and resuspended in lysis buffer [50 mM Tris-HCl, pH 6.8, 1 mM EDTA, pH 8.0, 2% sodium dodecyl sulfate (SDS), 100 mM Na_3VO_4]. The concentration of the total proteins was measured by a protein assay kit (Pierce, Rockford, USA) according to the manufacturer's protocol and was used for each Western blot analysis. The extracted proteins were separated by SDS-polyacrylamide gel electrophoresis (SDS-PAGE) on 12% polyacrylamide gels and were transferred to nitrocellulose membranes (Millipore, Billerica, USA) using standard methods. After incubation with a blocking buffer (PBS containing 5% bovine serum albumin) at room temperature, the nitrocellulose membranes were probed with the indicated antibody overnight at room temperature. The antibodies were used at the following dilutions and obtained from the indicated sources: goat anti-HCV NS3 antibody diluted 1:50 (Santa Cruz Biotechnology, Santa Cruz, USA); and rabbit anti-p44/42 MAPK antibody diluted 1:1000, rabbit anti-phosphor-p44/42 MAPK antibody diluted 1:200, rabbit anti-p38 MAPK antibody diluted 1:100, and mouse anti-phospho-p38 MAPK diluted 1:200 (Cell Signaling Technology, Boston, USA). Mouse anti α-tubulin antibody (1:2000, Santa Cruz Biotechnology) was used as a loading control. The membranes were incubated with secondary antibody (horseradish peroxidase-conjugated anti-mouse, anti-goat or anti-rabbit immunoglobulin G, 1:10,000 dilution; Amersham Biosciences, Piscataway, USA). Antigen-antibody complexes were visualized by enhanced chemiluminescence (Amersham Pharmacia Biotech, Buckinghamshire, UK). The relative density values were determined with UTHSCSA Image Tool 3.0 (University of Texas Medical School at San Antonio, USA).

Cell immunohistochemical staining

Cells were seeded on slides and incubated for 2 d and then fixed in acetone for 20 min at 4 ºC. Fixed cells were washed three times in PBS and non-specific proteins were blocked using non-immune serum (Zhongshan, Beijing, China) for 30 min at room temperature. Cells were incubated with the anti-HCV NS3 antibody overnight at room temperature, then washed twice in PBS. Cells were then incubated for 1 h with rabbit anti-goat immunoglobulin G-conjugated horseradish peroxidase diluted at 1:3000 (Zhongshan), followed by two washes in PBS. Cells were stained with diaminobenzidine reagent (Zhongshan).

Cell growth assay

For cell growth analysis, 1×10^5 cells were seeded onto 6-well plates in duplicate at day 0. Cells were daily trypsinized and live cells were counted after Trypan Blue straining. Triplicate wells were counted at each time point and the population doubling time was obtained from day 1 to day 7.

Anchorage-independent growth

A total of 2×10^3/ml cells were suspended in 0.3% agar containing Dulbecco's modified Eagle's medium and 10% fetal calf serum and overloaded onto a bottom layer of 0.7% agar in 6-well plates. After 4 weeks of culture, the morphology of transfected cells was analyzed microscopically. Colonies including more than 50 cells were scored and the efficiency of colony formation was determined. The experiment was repeated three times.

Tumor development in athymic nude mice

Sixteen nude mice (BALB/cA nude, females, 4–6 weeks old, 18–22 g; Shanghai Laboratorial Animal Center, Shanghai, China) were divided into four groups stochastically and inoculated subcutaneously in the right flank with pRcHCNS3/QSG, pRcCMV/QSG, or QSG7701 cells (1×10^7 cells in 0.2 ml PBS). HepG2 cells were used as the positive control. Tumor size and animal weight were measured weekly. The mice were killed and the tumors were removed 40 d after inoculation.

Immunohistochemistry

The fresh tumor tissue was formalin-fixed, paraffin-embedded and sectioned into 5 μm slices. Slices were mounted on poly-L-lysine-coated slides. The end section was stained with hemetoxylin-eosin to ensure that the lesion was still present in the serial sections. After deparaffinizaion, the slides were blocked with 3% hydrogen peroxide for 10 min and subjected to antigen retrieval with microwave in 10 mM citrate buffer for 15 min. The anti-HCV NS3 antibody was applied to the slides and incubated at room temperature overnight. After washing with PBS, the streptavidin-peroxidase kit (Zymed Laboratories, San Diego, USA) and diaminobenzidine chromogen were used to develop the stain. Immunohistochemical stains were interpreted as positive if at least 10% of the neoplastic cells showed intense immunoreactivity.

2-DE and image analysis

The cultured cells were harvested when they reached approximately 80% confluence, solubilized in a lysis buffer

containing 7 M urea, 4% CHAPS, 40 mM Tris, and 65 mM dithiothreitol, and centrifuged. The protein concentrations were determined using the protein assay kit. Three samples per cell strain were prepared from individual cell cultures. Samples were then loaded onto immobilized pH gradient strips (pH 3–10L, 240 mm×3 mm×0.5 mm) using an IPGphor isoelectric focusing cell (Amersham Biosciences). Second-dimension SDS-PAGE was carried out using the Ettan Dalt II system (Amersham Biosciences). 2-DE was carried out according to the method described by Gorg *et al*. [20]. After electrophoresis, the gels were visualized with a silver staining kit. All chemicals and equipment used for 2-DE were from Amersham Biosciences. The stained 2-DE gels were scanned with LabScan software (Amersham Biosciences) on an ImageScanner with a resolution of 300 dpi. The spot-intensity calibration, spot detection, background abstraction, matching, 1-D calibration, and the establishment of the average gel were carried out with ImageMaster 2D Elite 4.01 analysis software (Amersham Biosciences).

MALDI-TOF MS analysis

Protein spots were excised from preparative gels and transferred to siliconized Eppendorf tubes. One protein-free gel piece was treated in parallel as a negative control. Proteins were in-gel digested as previously described [21]. Briefly, the gel spots was destained in the destaining solution comprising 100 mM $Na_2S_2O_3$ and 30 mM $K_3Fe(CN)_6$ (1:1). The protein-containing spots were reduced in the reduction buffer (100 mM NH_4HCO_3 and 10 mM dithiothreitol) for 1 h at 57 ºC, and alkylated in the alkylation buffer (100 mM NH_4HCO_3 and 55 mM iodoacetamide) in the dark for 30 min at room temperature. The gel pieces were dried in a vacuum centrifuge. The dried gel pieces were incubated in the digestion solution (40 mM NH_4HCO_3, 9% acetonitrile, and 20 mg/ml trypsin) for 16 h at 37 ºC and mixed with α-cyano-4-hydroxy-cinnamic-acid matrix solution. A volume (1 μl) of the mixture containing α-cyano-4-hydroxy-cinnamic-acid matrix was loaded on a stainless steel plate and dried in the air. The samples were analyzed with an Applied Biosystems Voyager System 4307 MALDI-TOF Mass Spectrometer (ABI, Foster City, USA). The parameters were set up as follows: positive ion-reflector mode; accelerating voltage 20 kV; grid voltage 64.5%; mirror voltage ratio 1.12; N2 laser wavelength 337 nm; pulse width 3 ns; number of laser shots 50; acquisition mass range 1000–3000 Da; delay 100 ns; and vacuum degree 4×10^{-7} Torr. A trypsin-fragment peak served as the internal standard for mass calibration. A list of the corrected mass peaks was the peptide mass fingerprinting (PMF).

Bioinformatics analysis

Proteins were identified with PMF data by searching software PeptIdent (http://www.expasy.pku.edu.cn/) using a MASCOT Distiller, which can detect peaks by attempting to fit an ideal isotopic distribution to the experimental data. The searching parameters were set up as follows: mass tolerance 60.5 Da; number of missed cleavage sites allowed 1; cysteine residue modified as carbamidomethyl-cys; variable modifications oxidation (M); minimum number of matched peptides 5; species selected as *Homo sapiens* (human); peptide ion $[M+H]^+$; mass values monoisotopic; searching range within the experimental isoelectric point (pI) value±0.5 pH unit and experimental (molecular weight) MW±20%.

Statistical analysis

Results were analyzed using one-way ANOVA (SPSS version 11.0; SPSS, Chicago, USA) with $P<0.01$ considered to be significant.

Results

Detection of HCV NS3 cDNA in stable transfectants of pRcHCNS3/QSG cells

In order to detect HCV NS3 cDNA in stable transfectants of pRcHCNS3/QSG cells, total genomic DNA was extracted and subjected to PCR analysis. As shown in **Fig. 1**, a 257 bp fragment was specifically amplified from

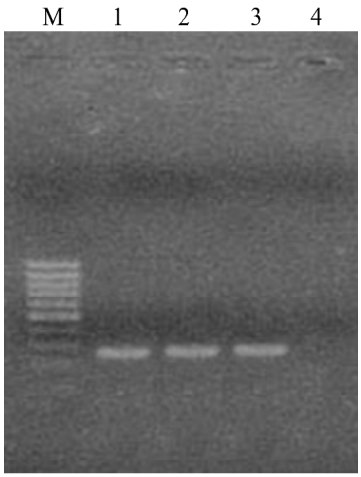

Fig. 1 DNA analysis from pRcHCNS3/QSG cells

The 257 bp fragment was specifically amplified from DNA of pRcHCNS3/QSG cells, but not from negative control. M, 100 bp marker; lanes 1–3, pRcHCNS3/QSG cells of passages 3, 6, and 9; lane 4, pRcCMV/QSG cells (negative control).

DNA of pRcHCNS3/QSG cells at passages 3, 6, and 9, but no fragment was amplified from DNA of the pRcCMV/QSG cells.

Detection of HCV NS3 protein expression in pRcHCNS3/QSG cells

In order to confirm the HCV NS3 protein expression in the stable transfectants of pRcHCNS3/QSG cells, the total proteins were extracted and subjected to Western blot and cell immunohistochemistry analysis. It was shown that the seven clones from pRcHCNS3/QSG cells all express HCV NS3 truncated protein that locates at 30 kDa (**Fig. 2**). Cell immunohistochemical staining showed that pRcHCNS3/QSG cells strongly expressed HCV NS3 truncated protein, and the positive signal was in the cytoplasm. The positive signal was found in the positive control group, but not in the negative control group (**Fig. 3**).

Cell growth assays

The effect of the HCV NS3 protein on cell growth was examined by the evaluation of proliferation rates and population doubling times. Growth curves were obtained by daily viable cell counts with the Trypan blue exclusion method. The plots were obtained from mean values of two independent clones of pRcCMV/QSG cell lines, parental QSG7701 cell lines and four different clones of pRcHCNS3/QSG cell lines. Duplicate wells from two independent experiments were counted at each time point. According to the daily cell counts, HCV NS3 transfectants showed a faster proliferation rate than the pRcCMV/QSG cells and parental QSG7701 (**Fig. 4**). Consistently, the population doubling time in pRcHCNS3/QSG cells was much shorter than that in pRcCMV/QSG cells and parental QSG7701 cells (12, 26, and 28 h, respectively; $P<0.01$ the former versus the latter two). HCV NS3 protein expression is suggested to be involved in the faster growth character of QSG7701 cell line.

Anchorage-independent growth

The ability of G418-resistant cells to grow anchorage independently was examined as follows. Cells (2×10^3 cells/ ml) were suspended containing 0.3% granulated agar and added over a layer of 0.7% agar in medium. Microscopic analysis of the transfected cells revealed colony formation at 4 weeks of culture in soft agar and anchorage-independent growth in the pRcHCNS3/QSG cells, whereas the pRcCMV/QSG and the parental cells showed no anchorage-independent growth under the same

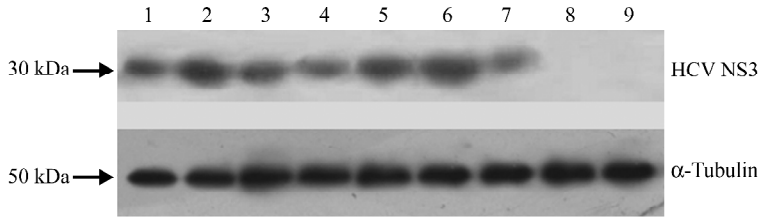

Fig. 2 Western blot analysis of hepatitis C virus non-structural protein 3 truncated protein expression

Lanes 1–7, subclones from pRcHCNS3/QSG; lane 8, pRcCMV/QSG (negative control) cells; lane 9, QSG7701 cells. α-Tubulin was used as the loading control.

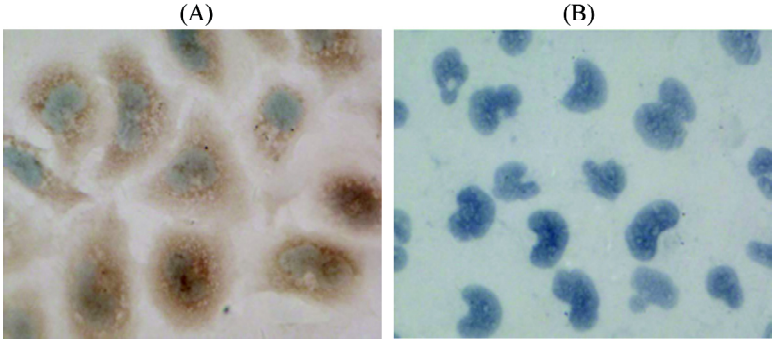

Fig. 3 Immunohistochemistry analysis (streptavidin-peroxidase) of hepatitis C virus non-structural protein 3 truncated protein expression in pRcHCNS3/QSG cells (A) and pRcCMV/QSG cells (B)

pRcHCNS3/QSG cells have been detected with positive signals in the cytoplasm. pRcCMV/QSG cells were used as negative control. Magnification, 400×.

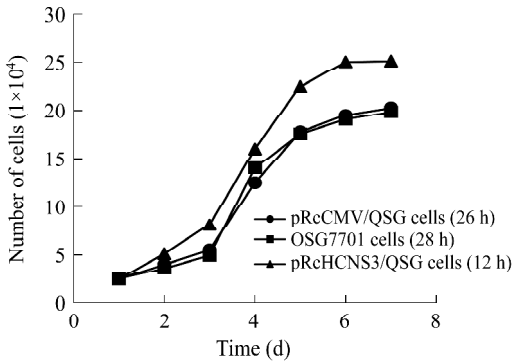

Fig. 4 Effect of hepatitis C virus non-structural protein 3 truncated protein expression on cell proliferation rates

Growth curves were obtained by daily viable cell counts and the population doubling times obtained from day 1 to day 7 are indicated.

conditions. The cloning efficiencies in pRcHCNS3/QSG cells, pRcCMV/QSG cells, and parental QSG7701 were 33 %, 1.46 %, and 1.11 %, respectively (P<0.01, the former versus the latter two) (data not shown).

Tumor development in nude mice

The tumorigenic potential of the transfectants was examined by inoculating nude mice with pRcHCNS3/QSG cells, pRcCMV/QSG cells, QSG7701 cells, or HepG2 cells. The first evidence of well-defined and distinct subcutaneous tumors appeared on day 15 in four mice inoculated with the pRcHCNS3/QSG cells. The mean tumor size and weight on day 40 were 3.08 cm^3 and 3.13 g, respectively. The HepG2 cells, as the positive control, also induced tumor in the nude mice. But no tumor developed in the mice inoculated with pRcCMV/QSG cells or QSG7701 cells until 40 d after inoculation. Macroscopically, the tumors induced by pRcHCNS3/QSG cells showed irregular yellow brown nodes and appeared to be encapsulated. Prominent necrosis could be seen on the cut surface. Microscopically, the tumor cells were similar to hepatocytes except for their heterogenesis and they were arranged in trabecular patterns with intervening sinusoids. Cancer cell nests with abundant coagulative necrosis were separated by fibrous tissue (**Fig. 5**). The tumors showed the histological characters of hepatocellular carcinoma. Immunohistochemical staining confirmed that the tumor tissue expressed HCV NS3 truncated protein and the positive signal was located in the cytoplasm (**Fig. 6**).

2-DE maps of the proteomes of pRcHCNS3/QSG and pRcCMV/QSG cells

2-DE maps were constructed for the proteomes of the

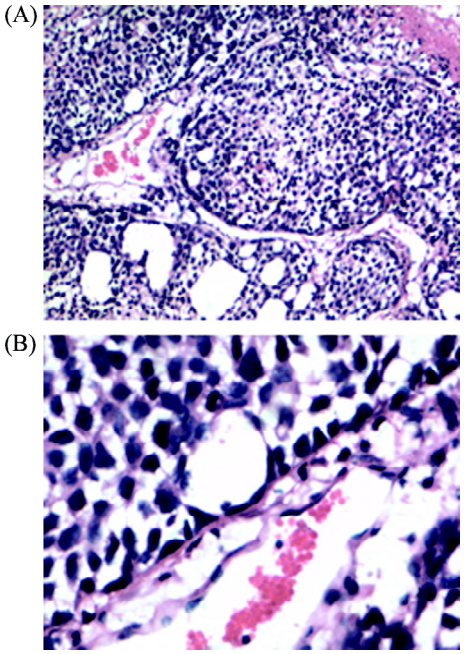

Fig. 5 Hepatocellular carcinoma induced by pRcHCNS3/QSG cells

Hematoxylin-eosin-stained section showing trabecular-arranged cancer cells and coagulative necrosis. Magnification, 100× (A), 400× (B).

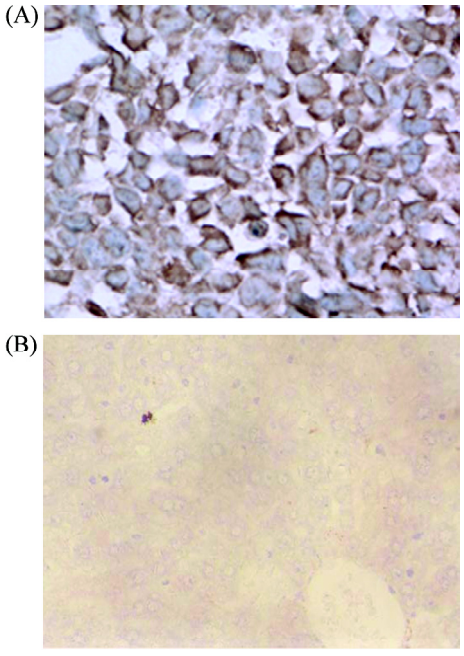

Fig. 6 Immunohistochemistry showing the hepatitis C virus non-structural protein 3 truncated protein expression in hepatocellular carcinoma induced by pRcHCNS3/QSG cells

(A) The positive signals are in the cytoplasm. (B) PBS substituting for the anti-HCV NS3 antibody was used to as negative control. Magnification, 400×.

pRcHCNS3/QSG and pRcCMV/QSG cells, as the establishment of a 2-DE protein map was a prerequisite for subsequent comparative proteomic studies. To validate the reproducibility, 2-DE was carried out in triplicate for the two kinds of cells. The image analysis showed that these 2-DE maps were reproducible. An average of 1183±77 spots were detected among three gels of pRcHCNS3/QSG cells and 1082±48 spots were matched with an average matching rate of 91.48%. For pRcCMV/QSG cells, a total of 1095±82 spots were detected, and 996±75 spots were matched with an average matching rate of 90.96%. A total of 100 well-resolved and matched spots among gels of pRcHCNS3/QSG cells were chosen randomly to calculate the deviation of the spot position. The spot positional deviation was 0.978±0.136 mm in the isoelectric focusing direction, and 1.225±0.315 mm in the SDS-PAGE direction. The well-resolved and reproducible 2-DE patterns of these cells are shown in **Fig. 7**. The 2-DE maps of pRcHCNS3/QSG cells were compared with the maps of pRcCMV/QSG cells, and 920±60 spots were matched.

MALDI-TOF MS analysis of the differential protein spots

A total of 21 differential protein spots, four spots expressed only in pRcHCNS3/QSG cells, the remaining spots expressed between pRcHCNS3/QSG cells and pRcCMV/QSG cells with at least a threefold discrepancy, were selected for MALDI-TOF MS-based PMF analysis

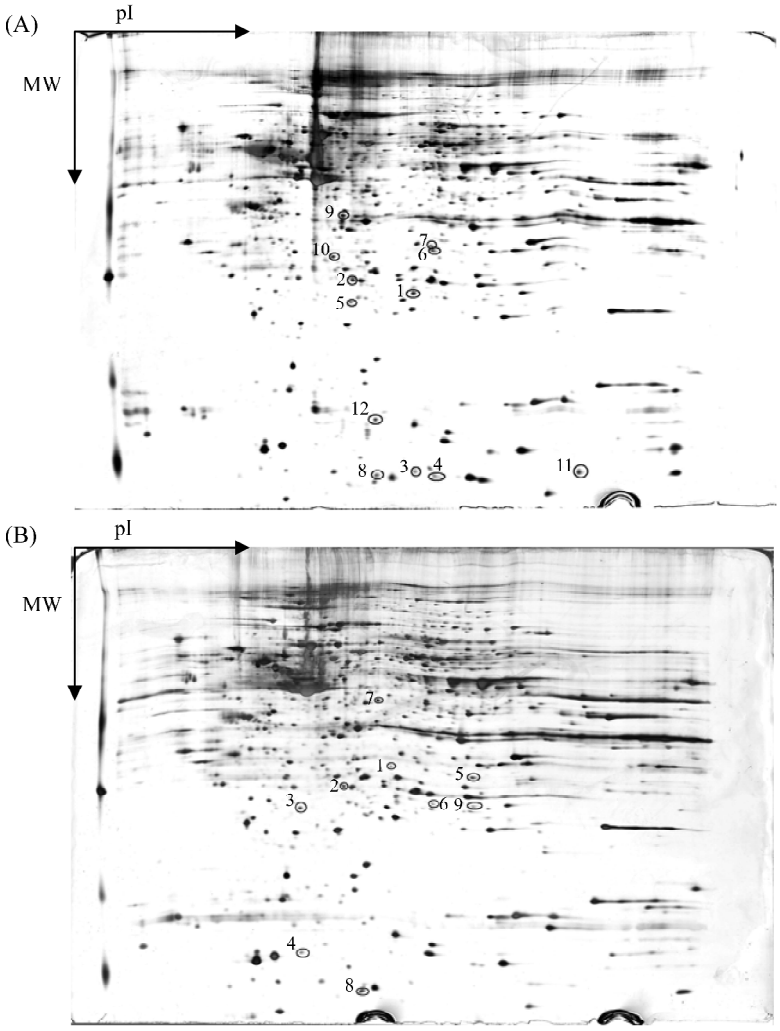

Fig. 7 2-D electrophoresis map of pRcHCNS3/QSG and pRcCMV/QSG cells

(A) pRcHCNS3/QSG cells. The numbered spots show proteins that were only expressed or overexpressed in pRcHCNS3/QSG cells. (B) pRcCMV/QSG cells. The numbered spots show the proteins that were only expressed or overexpressed in pRcCMV/QSG cells or down-expressed in pRcHCNS3/QSG cells. MW, mass weight; pI, isoelectric point.

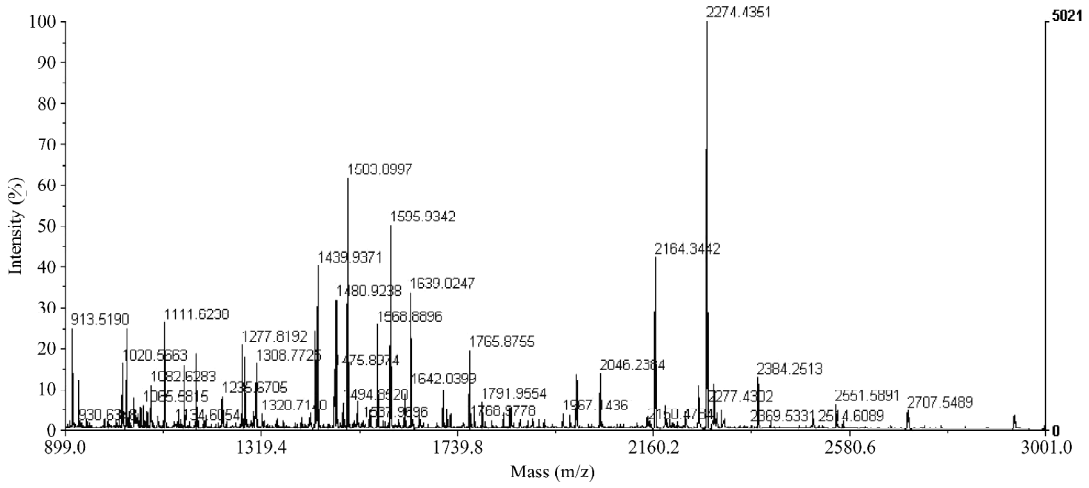

Fig. 8 Representative matrix-assisted laser desorption ionization-time of flight mass spectrum of protein spot NS1 in a 2-D electrophoresis map of pRcHCNS3/QSG cells

This peptide mass fingerprinting was identified as CHAIN 1:Follistatin by database search (Swiss-Prot, TrEMBL and National Center for Biotechnology Information databases).

[22]. These differential protein spots were excised from the silver-stained gels, and digested in-gel with trypsin. The PMF maps were obtained by MALDI-TOF MS, and calibrated with a trypsin auto-degraded peak (*m/z* 1993.9772 Da). **Fig. 8** shows the PMF maps of the spot NS1. The PMF data were used to search the Swiss-Prot, TrEMBL and National Center for Biotechnology Information databases with PeptIdent software. The resulting protein was determined by comprehensively comparing the corresponding experimental isoelectric point, Mr, the number of matched peptides, and the sequence coverage. Of the 21 protein spots, 15 differential proteins were identified by PMF. The data for all identified protein spots are shown in **Tables 1** and **2**. By using this approach, cellular signal proteins, immunity proteins, cell cycle proteins, cellular proliferation and apoptosis proteins, tumor infiltration and metastasis proteins, and metabolic proteins of liver were found to be differentially expressed in the pRcHCNS3/QSG and pRcCMV/QSG cells.

Western blot analysis

From the identified candidates, p44/42 and p38 were selected for Western blot analysis to validate the reliability of the identified results. As shown in **Figs. 9** and **10**, the expression of total p44/42 and p38 proteins in the pRcHCNS3/QSG cells was not distinctly different from these two proteins in the pRcCMV/QSG cells and QSG7701 cells, whereas phospho-p44/42 and phospho-p38 were up-regulated in pRcHCNS3/QSG cells compared to pRcCMV/QSG and QSG7701 cells. The experiments were repeated three times and carried out in three different stable cell clones. The expression changes of these selected proteins were consistent with 2-DE and silver-staining results. These results showed that the proteomic analysis of HCV NS3-transfected cells is convincing, and suggest that these proteins play roles in the cell transformation induced by HCV NS3.

Discussion

Here we studied the biological behaviors of QSG7701 cells constitutively expressing HCV NS3 protein to examine the role of the NS3 protein in cell proliferation. QSG7701 cells are immortally non-tumorigenic hepatocytes of human origin with hypotriploid phenotype. They came from liver tissue 6 cm from HCC [19]. After being transfected with HCV NS3, the cells grew rapidly, showed anchorage-independent growth in soft agar and induced significant tumor formation in nude mice. The tumors obtained from the nude mice showed the histological features of HCC and strongly expressed HCV NS3 protein. The present study indicated that QSG7701 cells acquire a transformed phenotype and become tumorigenic in nude mice after stably transfected with the HCV NS3 gene. Furthermore, the protein alteration induced by HCV NS3 was investigated by proteomics methods. Fifteen differentially-expressed protein spots were separated and identified by 2-DE and

Table 1 Characterized differentially-expressed proteins in pRcHCNS3/QSG cells compared to pRcCMV/QSG cells

Spot ID	AC ID	Peptides matched	pI	MW	Coverage (%)	Protein name or description
NS1	P19883	14/33	5.31	34754.26	51.4	CHAIN 1:Follistatin
NS2	Q96E17	8/44	5.09	25952.19	28.2	Ras-related protein Rab-3C
NS3	Q03403	8/25	5.21	11989.48	44.3	CHAIN 1:Trefoil factor 2
NS4	P56812	4/27	5.77	14285.08	36.8	Programmed cell death protein 5 (TFAR19 protein) (TF-1 cell apoptosis related gene-19 protein)
NS5	Q16890	4/4	5.45	22449.07	14.7	Tumor protein D53 (HD53) (D52-like 1)
NS6	O95433	5/10	5.41	38274.32	16.9	Activator of 90 kDa heat shock protein ATPase homolog 1 (AHA1) (p38) (HSPC323)
NS7	P15529-14	6/15	5.70	40692.81	12.9	Splice isoform I of membrane cofactor protein precursor (CD46 antigen) (trophoblast leucocyte common antigen) (TLX)
NS8	P17014	5/16	5.41	14688.68	17.4	p53 binding protein MDM2 (oncogene MDM2)
CMV1	P30279	6/26	5.06	33067.23	24.6	G_1/S-specific cyclin D2
CMV2	Q9HCU9	12/44	4.69	28460.65	33.7	Breast cancer metastasis suppressor-1
CMV3	Q99674	4/18	4.39	31976.53	21.3	Cell growth regulatory gene 11 protein (cell growth regulator with EF-hand domain 1)
CMV4	P00742	7/27	4.59	15725.25	51.1	CHAIN 1:Factor X light chain
CMV5	P30466	5/16	6.15	37609.64	13.6	CHAIN 1:HLA class I histocompatibility antigen
CMV6	P49675	6/18	–	–	27.0	Steroidogenic acute regulatory protein, mitochondrial precursor (StAR) (StARD1)
CMV7	Q14865	8/23	–	–	21.5	Modulator recognition factor protein 2 (Mrf-2)

AC, access; NS, non-structural; pI, isoelectric point. –, uncertain.

Table 2 Characterized functions of the identified differentially expressed proteins

Function category	pRcHCNS3/QSG cells	
	Up-expressed protein	Down-expressed protein
Cellular signal proteins	Ras, p38, HD53	None
Immunity proteins	CD46	MHC-1
Cell cycle proteins	MDM2	Cyclin D2
Cellular proliferation and apoptosis proteins	Follistatin, TFAR19	CGR11
Tumor infiltration and metastasis proteins	TFF2	BRSM1
Metabolic proteins of liver	None	StAR, Mrf-2, Factor X

MALDI-TOF MS-based PMF analysis. Some of the identified proteins with differential expression are regulatory proteins of signal transduction, cell cycle, and immune response. Others are proteins associated with cell proliferation and apoptosis, tumor infiltration and metastasis, and liver metabolism. Western blot analysis confirmed the increase of phospho-p44/42 and phospho-p38 protein was associated with transformed cells.

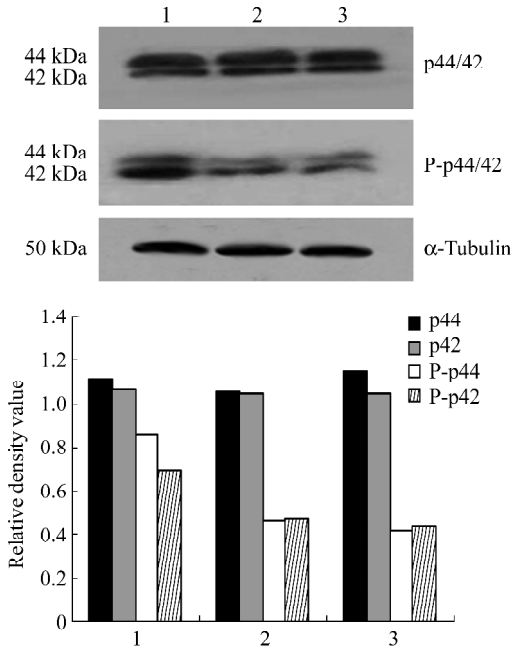

Fig. 9 Expression of total p44/42 and phospho- (p-)p44/42

1, pRcHCNS3/QSG cells; 2, pRcCMV/QSG cells; 3, QSG7701 cells. α-Tubulin was used as a loading control.

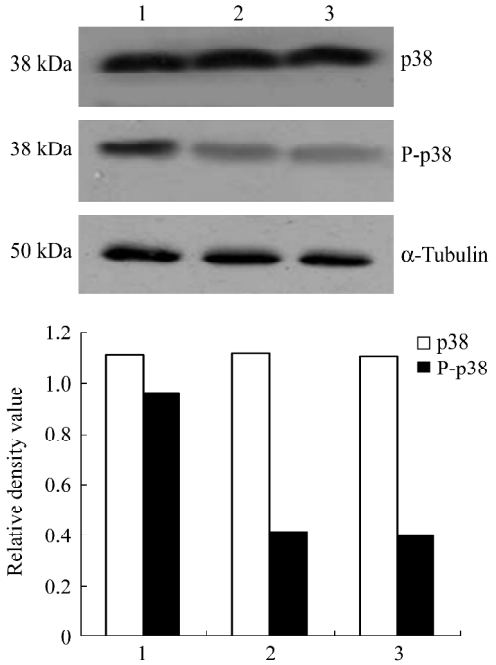

Fig. 10 Expression of total p38 and phospho- (p-)p38

1, pRcHCNS3/QSG cells; 2, pRcCMV/QSG cells; 3, QSG7701 cells. α-Tubulin was used as a loading control.

It has been shown that HCV replication and protein expression can be observed in HCC tissue [23]. HCV infection plays an important role in HCC development. As an RNA virus without any reverse transcriptase activity, HCV is replicated in the cytoplasm and does not integrate with the host genome. Various studies indicate that the interaction between the HCV protein and host cell has been involved in hepatocarcinogenesis.

As an important component of HCV, the role of the NS3 protein in cell proliferation and apoptosis has been previously suggested by studies with conflicting results. Consistent with the present results, these reports described the effect of the NS3 protein in the acceleration of cell proliferation. Sakamuro *et al*. [6] showed a promotion of cell proliferation and a transformation of cells by the HCV NS3 protein. Fujita *et al*. [8] reported HCV NS3 suppressed cell apoptosis, and Siavoshian *et al*. [11] showed HCV NS3 inhibited the growth of cells and arrested cells in the G_2/M phase of the cell cycle. Prikhod'ko *et al*. [12] regarded HCV NS3 as a pro-apoptotic protein. Unlike these studies, the present data were obtained by the HCV NS3 protein expression in a human hepatocyte cell line, QSG7701, which is biosynthetically and biochemically similar to human normal hepatocytes, thus being suitable for studying virus-cell interactions of hepatotropic viruses like HCV. Moreover, we examined the NS3 protein effect on cell proliferation in non-synchronized cell lines, which more appropriately reproduce conditions of the liver *in vivo*. Our study confirmed the effect of HCV NS3 on hepatocyte proliferation and malignant transformation.

Of the identified differentially-expressed proteins, Ras and p38 proteins were up-expressed in cells transfected with HCV NS3. Western blot analysis further confirmed that expression of phospho-p44/42 and phospho-p38 was stronger in HCV NS3 transfectants than in the negative and parallel controls. The Ras/Raf/MAPK pathway is regarded to have a close relation to HCV-associated HCC. Constitutive activation of the Ras/Raf/MAPK pathway is important for the transformation of mammalian cells [24, 25]. Indeed, studies have shown that HCC development and progression is associated with the activation of the Ras/Raf/MAPK pathway in humans and rodents [26,27]. Our laboratory also found that MAPK activity is higher in HCC than in adjacent non-cancerous lesions, suggesting a progression of HCC through Ras/Raf/MAPK activation [28]. Several reports have focused on the relationship between the HCV protein and the Ras/Raf/MAPK signal transduction pathway. Tsutsumi *et al*. [29] showed that the HCV core protein could activate extracellular signal-regulated kinase (ERK) and p38 MAPK in cooperation with ethanol in transgenic mice. Zhao *et al*. [30] reported that the HCV E2 protein specifically activated the MAPK/ERK pathway including downstream transcription factor ATF-

2 and greatly promoted cell proliferation. Park *et al*. [31] showed that the HCV NS5A protein modulated c-Jun N-terminal kinase and played a role in HCV pathogenesis. The HCV NS3 protein was reported to activate the MAPK signaling pathway JNK [15]. Interestingly, tumor protein D53 (HD53) was detected to be expressed only in HCV NS3 transfected cells. HD53 belongs to a tumor cell gene cluster strongly expressed in colon, ovarian and breast carcinoma cell lines [32]. HD53 proteins might have functions that are parallel or lie upstream of Raf kinases [33]. Combining these findings with our results, HCV NS3 might target various steps in the MAPK pathway that are involved in cell malignant transformation.

Other differentially-expressed proteins, such as MDM2 and cyclin D2, are proteins involved in the cell cycle. The promotion of cell cycle progression by MDM2 was mediated through p53 inhibition, and by regulating the pRb/E2F complex [34]. Endo *et al*. [35] found that MDM2 expression was significantly correlated with mutant p53 expression in human HCC. As a member of the D-type cyclins, cyclin D2 was implicated in cell cycle regulation, differentiation, and malignant transformation. Meyyappan *et al*. [36] suggested that, in addition to a role in promoting cell cycle progression, cyclin D2 might contribute to the induction and/or maintenance of a non-proliferative state. CD46 and MHC-I are immune-related proteins. CD46 expression was detected in most cancers including HCC [37]. Overexpression of CD46 on tumor cells might hamper the effect of immunotherapy with complement-activating monoclonal antibody. MHC-I antigen down-regulation or loss has been found in 16%–50% of malignant lesions in many malignancies with a poor prognosis of the disease and with reduced free interval and survival [38]. Follistatin, programmed cell death protein 5 (TFAR19) and cell growth regulatory gene 11 protein (CGR11) are proteins concerned with cellular proliferation and apoptosis. Rossmanith *et al*. [39] detected increased levels of follistatin mRNA in hepatocellular carcinoma compared to tumor-surrounding liver tissue and suggested that overexpression of follistatin might represent a unique strategy for hepatic tumors to overcome activin growth control. TFAR19 has a ubiquitous expression pattern and its expression in tumor cells enhances apoptosis triggered by growth factor or serum deprivation [40]. CGR11 was isolated using differential reverse transcription-PCR analysis of rat embryo fibroblast cells containing a temperature-sensitive p53 allele. Transfection assay experiments showed that CGR11 was able to inhibit growth in several cell lines [41]. Trefoil factor family 2 is a small peptide constitutively expressed in the gastric mucosa, where it plays a protective role in restitution of gastric mucosa. Trefoil factor family 2 expression might play a role in gastric cancer invasion and, as such, could be a useful target for therapeutic intervention [42]. Breast cancer metastasis suppressor-1 is a mediator of metastasis suppression in human breast carcinoma [43]. StAR, Mrf-2, and Factro X are metabolic proteins of liver. Elucidation of the precise function and mechanism involved in the carcinogensis of HCV awaits further analysis.

In conclusion, this study emphasizes the role and mechanism of the HCV NS3 protein in cell transformation. Our results gave some clues to elucidate the mechanism of HCC carcinogenesis. Further research on the relationship between HCV and these differentially-expressed proteins could provide the basis for searching potential molecular markers for virus-mediated HCC diagnoses, prognosis and therapy.

Acknowledgements

We thank Prof. TAKEGAMI for his generous gift of plasmid pRcHCNS3-5'.

References

1 Houghton M. Strategies and prospects for vaccination against the hepatitis C viruses. Curr Top Microbiol Immunol 2000, 242: 327–339
2 Iino S. Natural history of hepatitis B and C virus infections. Oncology 2002, 62: 18–23
3 Cerni A, Chisari FV. Pathogenesis of chronic hepatitis: Immunological features of hepatic injury and viral persistence. Hepatology 1999, 30: 595–601
4 Grakoui A, Wychowski C, Lin C, Feinstone SM, Rice CM. Expression and identification of hepatitis C virus polyprotein cleavage products. J Virol 1993, 67: 1385–1395
5 Gallinari P, Brennan D, Nardi C, Brunetti M, Tomei L, Steinkuhler C, de Francesco R. Multiple enzymatic activities associated with recombinant NS3 protein of hepatitis C virus. J Virol 1998, 72: 6758–6769
6 Sakamuro D, Furukawa T, Takegami T. Hepatitis C virus nonstructural protein NS3 transforms NIH 3T3 cells. J Virol 1995, 69: 3893–3896
7 Kwun HJ, Jung EY, Ahn JY, Lee MN, Jang KL. p53-Dependent transcriptional repression of p21(waf1) by hepatitis C virus NS3. J Gen Virol 2001, 82: 2235-2241
8 Fujita T, Ishido S, Muramatsu S, Itoh M, Hotta H. Suppression of actinomycin D-induced apoptosis by the NS3 protein of hepatitis C virus. Biochem Biophys Res Commun 1996, 229: 825–831
9 Zemel R, Gerechet S, Greif H, Bachmatove L, Birk Y, Golan-Goldhirsh A, Kunin M *et al*. Cell transformation induced by hepatitis C virus NS3 serine protease. J Viral Hepat 2001, 8: 96–102
10 Zemel R, Berdichevsky Y, Bachmatov L, Z Benhar I, Tur-Kaspa R. Inhibition of hepatitis C virus NS3-mediated cell transformation by recombinant intracellular antibodies. J Hepatol 2004, 40: 1000–1007
11 Siavoshian S, Abraham JD, Kieny MP, Schuster C. HCV core, NS3, NS5A and NS5B proteins modulate cell proliferation independently from p53 ex-

pression in hepatocarcinoma cell lines. Arch Virol 2004, 149: 323–336
12 Prikhod'ko EA, Prikhod'ko GG, Siegel RM, Thompson P, Major ME, Cohen JI. The NS3 protein of hepatitis C virus induces caspase-8-mediated apoptosis independent of its protease or helicase activities. Virology 2004, 329: 53–67
13 Borowski P, Heiland M, Feucht H, Laufs R. Characterisation of non-structural protein 3 of hepatitis C virus as modulator of protein phosphorylation mediated by PKA and PKC: Evidences for action on the level of substrate and enzyme. Arch Virol 1999, 144: 687–701
14 Borowski P, Resch K, Schmitz H, Heiland M. A synthetic peptide derived from the non-structural protein 3 of hepatitis C virus serves as a specific substrate for PKC. Biol Chem 2000, 381: 19–27
15 Hassan M, Ghozlan H, Abdel-Kader O. Activation of c-Jun NH2-terminal kinase (JNK) signaling pathway is essential for the stimulation of hepatitis C virus (HCV) non-structural protein 3 (NS3)-mediated cell growth. Virology 2005, 333: 324–336
16 Feng D, Cheng R, Ouyang X, Zheng H, Tsutomu T. Hepatitis C virus nonstructural protein NS(3) and telomerase activity. Chin Med J (Engl) 2002, 115: 597–602
17 Kim W, Oe Lim S, Kim JS, Ryu YH, Byeon JY, Kim HJ, Kim YI *et al*. Comparison of proteome between hepatitis B virus- and hepatitis C virus-associated hepatocellular carcinoma. Clin Cancer Res 2003, 9: 5493–5500
18 Le Naour F, Brichory F, Misek DE, Bréchot C, Hanash SM, Beretta L. A distinct repertoire of autoantibodies in hepatocellular carcinoma identified by proteomic analysis. Mol Cell Proteomics 2002, 1: 197–203
19 Zhu DH, Wang JB. The culture of HCC host hepatocyte QSG7701 cell line and as compared with hepatocarcinoma cell. Zhongliu Fangzhi Yanjiu 1979, 5: 7–9
20 Gorg A, Obermaier C, Boguth G, Harder A, Scheibe B, Wildgruber R, Weiss W. The current state of two-dimensional electrophoresis with immobilized pH gradients. Electrophoresis 2000, 21: 1037–1053
21 Chen P, Xie JY, Liang SP. Identification of protein spots in silver-stained two-dimensional gels by MALDI-TOF mass peptide map analysis. Acta Biochim Biophys Sin 2000, 32: 387–391
22 Kim J, Kim SH, Lee SU, Ha GH, Kang DG, Ha NY, Ahn JS *et al*. Proteome analysis of human liver tumor tissue by two-dimensional gel electrophoresis and matrix assisted laser desorption/ionization-mass spectrometry for identification of disease-related proteins. Electrophoresis 2002, 23: 4142–4156
23 Ohishi M, Sakisaka S, Harada M, Koga H, Taniguchi E, Kawaguchi T, Sasatomi *et al*. Detection of hepatitis-C virus and hepatitis-C virus replication in hepatocellular carcinoma by *in situ* hybridization. Scand J Gastroenterol 1999, 34: 432–438
24 Pinkas J, Leder P. MEK1 signaling mediates transformation and metastasis of EpH4 mammary epithelial cells independent of an epithelial to mesenchymal transition. Cancer Res 2002, 62: 4781–4790
25 Hamad NM, Elconin JH, Karnoub AE, Bai W, Rich JN, Abraham RT, Der CJ *et al*. Distinct requirements for Ras oncogenesis in human versus mouse cells. Genes Dev 2002, 16: 2045–2057
26 Zhu J, Leng X, Dong N, Liu Y, Li G, Du R. Expression of mitogen- activated protein kinase and its upstream regulated signal in human hepatocellular carcinoma. Zhonghua Waike Zazhi 2002, 40: 1–16
27 Ostrowski J, Woszczynski M, Kowalczyk P, Wocial T, Hennig E, Trzeciak L, Janik P *et al*. Increased activity of MAP, p70S6 and p90rs kinases is associated with AP-1 activation in spontaneous liver tumours, but not in adjacent tissue in mice. Br J Cancer 2002, 82: 1041–1050
28 Feng DY, Zheng H, Tan Y, Cheng RX. Effect of phosphorylation of MAPK and Stat3 and expression of c-fos and c-jun proteins on hepatocarcinogenesis and their clinical significance. World J Gastroenterol 2001, 7: 33–36
29 Tsutsumi T, Suzuki T, Moriya K, Shintani Y, Fujie H, Miyoshi H, Matsuura *et al*. Hepatitis C virus core protein activates ERK and p38 MAPK in cooperation with ethanol in transgenic mice. Hepatology 2003, 38: 820–828
30 Zhao LJ, Wang L, Ren H, Cao J, Li L, Ke JS, Qi ZT. Hepatitis C virus E2 protein promoted human hepatoma cell proliferation through the MAPK/ERK signaling pathway via cellular receptors. Exp Cell Res 2005, 305: 23–32
31 Park KJ, Choi SH, Choi DH, Park JM, Yie SW, Lee SY, Hwang SB. Hepatitis C virus NS5A protein modulates c-Jun N-terminal kinase through interaction with tumor necrosis factor receptor-associated factor 2. J Biol Chem 2003, 278: 30711–30718
32 Ross DT, Scherf U, Eisen MB, Perou CM, Rees C, Spellman P, Iyer V *et al*. Systematic variation in gene expression patterns in human cancer cell lines. Nat Genet 2000, 24: 227–235
33 Boutros R, Bailey AM, Wilson SH, Byrne JA. Alternative splicing as a mechanism for regulating 14-3-3 binding: Interactions between hD53 (TPD52L1) and 14-3-3 proteins. J Mol Biol 2003, 332: 675–687
34 Levav-Cohen Y, Haupt S, Haupt Y. Mdm2 in growth signaling and cancer. Growth Factors 2005, 23: 183–192
35 Endo K, Ueda T, Ohta T, Terada T. Protein expression of MDM2 and its clinicopathological relationships in human hepatocellular carcinoma. Liver 2000, 20: 209–215
36 Meyyappan M, Wong H, Hull C, Riabowol KT. Increased expression of cyclin D2 during multiple states of growth arrest in primary and established cells. Mol Cell Biol 1998, 18: 3163–3172
37 Fishelson Z, Donin N, Zell S, Schultz S, Kirschfink M. Obstacles to cancer immunotherapy: Expression of membrane complement regulatory proteins (mCRPs) in tumors. Mol Immunol 2003, 40: 109–123
38 Chang CC, Campoli M, Ferrone S. HLA class I defects in malignant lesions: What have we learned? Keio J Med 2003, 52: 220–229
39 Rossmanith W, Chabicovsky M, Grasl-Kraupp B, Peter B, Schausberger E, Schulte-Hermann R. Follistatin overexpression in rodent liver tumors: A possible mechanism to overcome activin growth control. Mol Carcinog 2002, 35: 1–5
40 Liu H, Wang Y, Zhang Y, Song Q, Di C, Chen G, Tang J *et al*. TFAR19, a novel apoptosis-related gene cloned from human leukemia cell line TF-1, could enhance apoptosis of some tumor cells induced by growth factor withdrawal. Biochem Biophys Res Commun 1999, 254: 203–210
41 Madden SL, Galella EA, Riley D, Bertelsen AH, Beaudry GA. Induction of cell growth regulatory genes by p53.Cancer Res 1996, 56: 5384–5390
42 Dhar DK, Wang TC, Maruyama R, Udagawa J, Kubota H, Fuji T, Tachibana M *et al*. Expression of cytoplasmic TFF2 is a marker of tumor metastasis and negative prognostic factor in gastric cancer. Lab Invest 2003, 83: 1343–1352
43 Seraj MJ, Samant RS, Verderame MF, Welch DR. Functional evidence for a novel human breast carcinoma metastasis suppressor, BRMS1, encoded at chromosome 11q13. Cancer Res 2000, 60: 2764–2769

Edited by
Mohamed HASSAN